Biosensors and Bioelectronics 68 (2015) 404–412

Contents lists available at ScienceDirect

Biosensors and Bioelectronics

journal homepage: www.elsevier.com/locate/bios

Liquid crystal-based glucose biosensor functionalized with mixed PAA and QP4VP brushes

Mashooq Khan, Soo-Young Park*

School of Applied Chemical Engineering, Kyungpook National University, #1370 Sangyuk-dong, Buk-gu, Daegu 702-701, South Korea

ARTICLE INFO

Article history:
Received 9 December 2014
Accepted 9 January 2015
Available online 10 January 2015

Keywords:
Biosensor
Mixed brushes
Glucose
Liquid-crystal
5CB
TEM

ABSTRACT

4-Cyano-4′-pentylbiphenyl (5CB) in a transmission electron microscopy (TEM) grid was developed for glucose detection by coating with a monolayer of mixed polymer brushes using poly(acrylicacid-*b*-4-cynobiphenyl-4′-oxyundecylacrylate) (PAA-*b*-LCP) and quaternized poly(4-vinylpyridine-*b*-4-cynobiphenyl-4′-oxyundecylacrylate) (QP4VP-*b*-LCP) (LCP stands for liquid crystal polymer) at the 5CB/aqueous interface. The resultant 5CB in TEM grid was functionalized with the PAA and QP4VP brushes, which were strongly anchored by the LCP block. The PAA brush rendered the 5CB/aqueous interface pH-responsive and the QP4VP brush immobilized glucose oxidase (GOx) through electrostatic interactions without the aid of coupling agents. The glucose was detected through a homeotropic-to-planar orientational transition of the 5CB observed through a polarized optical microscope (POM) under crossed polarizers. The optimum immobilization with a 0.78 μM GOx solution on the dual-brush-coated TEM grid enabled glucose detection at concentrations higher than 0.5 mM with response times shorter than 180 s. This TEM grid glucose sensor provided a linear response of birefringence of the 5CB to glucose concentrations ranging from 0.5 to 11 mM with a Michaelis–Menten constant (K_m) of 1.67 mM. This new and sensitive glucose biosensor has the advantages of low production cost, simple enzyme immobilization, high enzyme sensitivity and stability, and easy detection with POM, and may be useful for prescreening the glucose level in the human body.

1. Introduction

Enzyme immobilization is a key factor in developing efficient biosensors with appropriate properties such as good operational and storage stability, high sensitivity, high selectivity, short response time, and high reproducibility. Immobilized enzymes must maintain their structure and function to retain biological activity, remain tightly bound, and not be desorbed during biosensing. Moreover, an ideal biosensor has to be stable for long-term application. The immobilization method affects the activity and stability of enzymatic biosensors. Factors such as accuracy of measurements, sensor-to-sensor reproducibility, and operational lifetimes are significantly influenced by enzyme stability. Intensive efforts have been made to develop successful immobilization strategies such as entrapment, physical adsorption, cross-linking, affinity, and covalent bonding to obtain high performance biosensors. Each immobilization method presents merits and demerits (Sassolas et al., 2012). Whether the biosensor application requires maximum sensitivity or stability determines which enzyme immobilization method is best. Reproducibility, cost, and difficulty also require consideration. Among the immobilization methods, covalent coupling is popular, and is carried out through the initial activation of support using coupling agents. However, the use of toxic coupling agents requires specific activating groups on the support surface, activation of the surface groups, replacement of the activating groups with enzymes, alteration of enzyme 3D structures, and chemical modification of enzymes, which make this method difficult (Liu et al., 2012; Rad et al., 2011; Rahman et al., 2010; Sassolas et al., 2012; Tischer and Wedekind, 1999; Zhu et al., 2012).

Depending on the pH of the enzyme solution, which controls the charge by an isoelectric point, and the surface charges of the substrate, the anionic or cationic surface can act as a support for immobilization of enzymes via electrostatic interactions (Mateo et al., 2007). Previously, both anionic and cationic metal ion exchangers were used for the immobilization of enzymes that retained the enzymatic activity and stability under optimal as well as non-optimal conditions (Nahalka et al., 2003). However, in these cases, the enzymes needed to contain imidazole residues or histidine tags which can act as ligands for metal ions (Hanefeld et al., 2009).

Polyelectrolytes (PEs), such as poly(acrylicacid)(PAA), quaternized poly(4-vinylpyridine) (QP4VP), poly(dimethylaminoethylmethacrylate)

* Corresponding author.
E-mail address: psy@knu.ac.kr (S.-Y. Park).

http://dx.doi.org/10.1016/j.bios.2015.01.023
0956-5663/

(PDMAEA), and poly(styrenesulfonate) (PSS) brushes have been applied towards biosensors through adsorption of proteins with liquid–crystal-filled transmission electron microscopy (TEM) grid cells (Lee et al., 2010; Omer et al., 2014a; Omer et al., 2014b; Omer and Park, 2014; Tan and Wang, 2011). We found that all PEs can adsorb oppositely charged proteins. Strong PEs such as QP4VP (cationic) and PSS (anionic) adsorbed proteins regardless of pH, while adsorption on weak PEs such as PAA (anionic) and PDMAEA (cationic) was pH-dependent because the charged states of the weak PEs depend on the protonation (for cationic PE) or deprotonation (for anionic PE) of the pendant groups below or above their pKa values. Since enzymes are proteins, they can be adsorbed on the PEs.

Research on mixed PE (MPE) brushes composed of two oppositely charged polymers grafted on the same substrate have been directed towards the fabrication of switchable hydrophobic/hydrophilic smart surfaces, Pickering emulsions, environmentally responsive lithography, and transport of particles across liquid–liquid interfaces (Zhao and Zhu, 2009). Self-assembled monolayers, photo-initiated free radical polymerization, photo etching, surface patterning, and imprinted masking layers have been used to synthesize MPE brushes (Tokarev and Minko, 2009). However, these methods need sophisticated chemical reactions or polymerization on the substrate and are not suitable for introducing MPE onto liquid crystals. Thus, a simple and convenient means for functionalization of the liquid–crystal-filled TEM grid cells with mixed brushes is highly desirable for biosensor development (Price et al., 2011). The properties of the MPE brushes can be tuned by varying the brush density, surface charges, chemical composition, addition of salts, and friction of the polymer (Draper et al., 2004; Wei et al., 2013). Thus, owing to their tuning properties, smart responses, and higher capacities for enzyme immobilization, (Jain et al., 2009) MPE brushes can be applied towards developing biosensors.

The choice of mixed brushes is crucial for application to biosensors. QP4VP is a strong PE that carries positive charges at any pH and can form strong ionic interactions with negatively charged enzymes above their isoelectric points (PIs). Also, it is promising for enzyme immobilization because QP4VP can expand to several times its initial thickness in aqueous solution, which facilitates binding of large biomolecules (Jain et al., 2009). PAA is a weak PE and its chain conformation and charge state is pH-dependent. In our previous study, glucose oxidase (GOx) which is immobilized covalently on the PAA-coated 4-cyano-4′-pentylbiphenyl (5CB) (a nematic liquid crystal at room temperature) in a TEM grid ($TEM_{PAA\text{-}GOx}$) showed enhanced glucose detection at the 5CB/aqueous interface. The small amount of glucose in solution was detected through a homeotropic-to-planar (H-P) orientational change of the 5CB observed under a polarized optical microscope (POM).(Khan and Park, 2013) This H-P change was attributed to a change in the local pH caused by the GOx-catalyzed oxidation of glucose as shown in Scheme 1. This mode of detection has several advantages such as low interference from other blood components (hemoglobin, ascorbic acid, uric acid etc.), easy fabrication of sensor cells, and simple detection (Khan and Park, 2013). However, the problems arising with covalent immobilization of enzyme and long term stability of the biosensor are needed to be resolve.

In this study, MPE brushes of QP4VP and PAA on the 5CB in a TEM grid were introduced for enzyme immobilization through

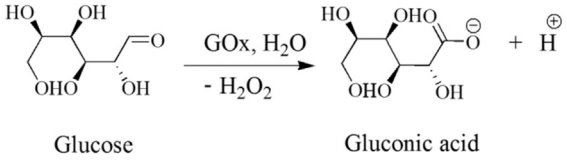

Scheme 1. GOx-catalyzed oxidation of glucose .

electrostatic interactions and glucose detection by pH-dependent charge state, respectively, with quaternized poly(4-vinylpyridine-b-4-cynobiphenyl-4′-oxyundecylacrylate) (QP4VP-*b*-LCP) and poly (acrylicacid-b-4-cynobiphenyl-4′-oxyundecylacrylate) (PAA-*b*-LCP) strongly anchoring in the 5CB in TEM grid. The ionic immobilization of GOx to QP4VP chains and the pH responsiveness of the PAA at the 5CB/aqueous interface were coupled to fabricate a glucose biosensor by coating 5CB in the TEM grid with a monolayer of PAA-*b*-LCP and QP4VP-*b*-LCP (TEM_{mixed}) at the 5CB/aqueous interface. A simple ionic immobilization without any chemical modification in this study retains the enzyme structure for a long period of time, is not time-consuming, and also avoids the use of other expensive reagents. The glucose was detected from an H-P transition of the 5CB, which occurred through protonation of the PAA chains. This TEM grid glucose sensor was tested for stability, enzyme activity, and sensitivity towards glucose detection.

2. Experimental

2.1. Materials

Microscope glass slides (Paul Marienfeld GmbH & Co. KG, Germany) was cleaned using piranha solution (***caution***: piranha solution is extremely corrosive and must be handled carefully), washed subsequently with distilled water, and dried under nitrogen. Copper TEM specimen grids (G75, grid hole width of 285 μm, pitch of 340 μm, bar width of 55 μm, size of 3.05 mm, and thickness of 18 μm) were purchased from Ted Pella, Inc. GOx (E.C. 1.1.3.4) from *Aspergillus niger* was obtained from Sigma-Aldrich as a salt-free lyophilized powder with a specific activity of $>100{,}000$ unit/g and a molecular weight of 1.6×10^5 g/mol. D-(+)-Glucose (Sigma), *N*-(3-dimethylaminopropyl)-*N*-ethylcarbodiimide hydrochloride (EDC·HCl, Sigma-Aldrich), *N*-hydroxysulfosuccinimide sodium salt (NHS, Sigma-Aldrich), sodium chloride (Aldrich), trifluoroacetic acid (TFA, Aldrich, 99%), 5CB (TCI, 100%), octadecyltrichlorosilane (OTS), methanol (Aldrich), dichloromethane (DCM, Aldrich), yeast extracts (Sigma), ascorbic acid (Fluka), and hemoglobin human (Sigma) were used as received. PAA-*b*-LCP and QP4VP-*b*-LCP were synthesized using the method reported previously (Khan et al., 2011; Lee et al., 2010). The number average molecular weights (M_ns) of PAA (11 K)-*b*-LCP (5 K) and QP4VP (16 K)-*b*-LCP (5.2 K) are given in parentheses, and their poly disperity indices (M_w/M_n) are 1.14 and 1.17, respectively (for example, 11 K is 11,000 g/mole).

2.2. Monolayer formation

The monolayer experiments were performed with a Langmuir–Blodgett (LB) KSV Layer builder (KSV Instruments Ltd., AAA100178, Finland) connected to a KSV mini-micro trough (17×5 cm^2), which was surrounded by an environmental chamber. The surface pressure of the monolayer at the air/liquid interface was measured using a Wilhelmy plate attached to a microbalance at room temperature. PAA-*b*-LCP was dissolved in dioxane and kept at 60 °C for two days. Subsequently, toluene was added to the dioxane solution to obtain a dioxane to toluene ratio of 6/4 (v/v) and a final concentration of 1 mg/mL. QP4VP-*b*-LCP was dissolved in distilled water (1 mg/mL). For the formation of the monolayer, a fixed volume of the PAA-*b*-LCP solution ($\nu_1=200$ μL) was dropped on the 1 M NaCl subphase and then a known volume of the QP4VP-*b*-LCP solution (ν_2) was immediately dropped on the subphase at zero surface pressure (π). Various amounts of ν_2 (20, 30, 40, 50, 60, 70, 80, and 100 μL) were tested to find the optimum ratio. Different concentrations of the NaCl solution ($C_{NaCl}=0.2$, 0.5, 0.75, and 1 M) were used as the subphase. One hour after monolayer formation,

the monolayer was compressed, expanded, and compressed again at a rate of 3 mm/min to achieve equilibrium. Fig, SI 1 shows the LB isotherm curve of the mixed QP4VP-*b*-LCP/PAA-*b*-LCP monolayer on a 1 M NaCl solution as the subphase. The surface pressure slowly increases until 50 mm^2 and then increases rapidly as the area is decreased further, indicating that a monolayer was formed on the subphase. The areal density of the monolayer was set at 36 mm^2 (π=~45 mN/m) in the region of a liquid-expanded phase of the monolayer (Osvaldo and Oliveira, 1992).

2.3. Device fabrication

The flow cell used in this study was prepared by the method reported in our previous study (Khan and Park, 2013). Briefly, microscope glass slides were cleaned and coated with OTS to align the 5CB perpendicular to the glass surface inducing homeotropic orientation. A TEM grid was placed on the surface of the 12×8 mm^2 OTS-coated glass that was glued to another glass slide with epoxy. A 1 μL drop of 5CB was placed on a TEM grid using a 5 μL glass syringe (HAMILTON Co., Reno, Nevada, USA). The excess 5CB was removed with a capillary tube to obtain a uniform thin film with ~18 μm thickness. To transfer the PAA-*b*-LCP/QP4VP-*b*-LCP monolayer onto the surface of 5CB in the TEM grid, the TEM grid filled with 5CB was inserted slowly into the LB bath with the TEM grid side down, coming to rest on a silicon spacer (2 mm thick) attached to a glass slide in the LB bath. The two glass slides spaced with silicon rubber were then clipped with binder clips. The internal volume of the flow cell was 0.4 mL. The inlet and outlet ports for exchanging the solutions were made with syringe needles punched through the silicon rubber. Fig. SI 2 shows the schematic and actual photograph of the flow cell.

2.4. Labeling and immobilization of GOx

The labeling of the GOx was carried out following a slight modification of a method reported elsewhere. Briefly, GOx was dissolved in phosphate buffered saline (PBS) buffer (pH=7) in a reaction vial to obtain a 20 μM solution into which the chemical coupling agents, EDC · HCl and NHS, were added and kept for 1 h at 4 °C to activate the carboxyl group in GOx. Subsequently, 1 mg of Rhodamin6G was added and stirred for 12 h at room temperature. A saturated aqueous ammonium sulfate solution (0.5 g/mL) was added dropwise to the mixture. The labeled GOx (GOx_{rhd6G}) was precipitated and centrifuged twice at 5000 rpm for 20 min. The supernatant was then removed by filtration and the filtered GOx_{rhd6G} powder was dried under vacuum. The UV–vis spectrum of the GOx_{rhd6G} (Fig. SI 3b) solution shows absorbance peaks at 526 and 276 nm, which can be attributed to Rhodamin 6 G (Fig. SI 3a) and GOx (Fig. SI 3c), respectively, indicating that GOx was successfully labeled. The electrostatic immobilization of GOx to the QP4VP chains on the 5CB in the TEM grid was carried out by injecting 3 mL of a 20 μM GOx solution into the flow cell. The amount of immobilized GOx was determined from the UV–visible spectrum. The calibration curve for the GOx (Fig. SI 4) aqueous solution was obtained in the range of 0–6 μM at a maximum absorbance wavelength (λ_{max}) of 276 nm. The amount of immobilized GOx (GOx_{imb}) was calculated from the difference in the GOx solution concentration before and after immobilization.

2.5. Practical analysis

In order to test the $TEM_{mixed\text{-}GOx}$ grid sensor for glucose detection in a sample, a complex mixture of yeast extracts (YE) (1 mg/mL), hemoglobin (5 mM), ascorbic acid (AA) (0.1 mM) and glucose (0.3, 0.5, and 2 mM) were prepared. The results of the $TEM_{mixed\text{-}GOx}$ sensor were compared with a standard high performance liquid chromatography (HPLC) technique. The YE is the common name for various forms of processed yeast products made by extracting the body cell contents and commonly used as food additives or flavorings and nutrients for diabetes and high cholesterol. YE was used for practical analysis because it contains all ingredients of the blood such as saturated and unsaturated fat, sodium, potassium, magnesium, chromium, carbohydrates sugar, protein and vitamin B-complex (Anderson, 1997) and may mimic the contents of a real blood sample with the addition of hemoglobin, AA and glucose. Fig. SI 5 shows the HPLC chromatograms of YE, glucose, and a YE/glucose mixture. The chromatogram of the YE does not show a peak at retention time (RT)= 9.75 min for glucose but that of the YE/glucose mixture exhibits a characteristic peak of glucose at RT=9.75 min confirming that YE does not have any glucose and the YE/glucose mixture can be used as a standard sample for demonstrating the practical analysis of the $TEM_{mixed\text{-}GOx}$ sensor.

2.6. Instrumentation

Images and videos of the TEM grid cells under a POM (Leitz, ANA-006**,** Germany) with a crossed polarizer state were recorded using a CCD camera (Samwon, STC-TC83USB, Korea). The UV–visible spectra were obtained using a UV–visible spectrophotometer (Shimadzu, 2401, Japan). The GOx_{rhd6G}on the TEM grid was confirmed by fluorescence microscopy (Nikon Eclipse, E600POL, Japan) and their fluorescence spectra were recorded with a high resolution spectrometer (HR4000, Ocean Optics, Inc., Japan) attached to a fluorescence microscope. The HPLC analysis was carried out using HPLC instrument (Waters Co. Model 600E) with a column (Sugar-Pak I (6.5 × 300 mm)) and a refractive index detector (RI, Model 410). Ca-EDTA buffer (50 mg Ca-EDTA/1 L dH2O) was used for the mobile phase with a flow rate of 0.5 mL/min at 90 °C in the column. The grey scale intensities (GI) of the video frames were calculated using Adobe Photoshop CS5 software. The optical birefringence (Δn) was measured using a tilting compensator (2073 K, equipped with a calcite compensator plate, Leitz, Germany) with source light intensity at 50% of full illumination. At the 0 position of the compensator, the crystal axis was parallel to the polarizer axis. Optical birefringence, Δn, is defined as Γ/d, where Γ is the phase difference and d is the sample thickness (18,000 nm). The Γ was measured from the tilting angle (2i) using the equation, $\Gamma = 10^4 f(2i) \times (C/10^4)$ where $f(2i)$ is tabulated in the instrument manual and c is the compensator constant (4.54×10^4). The measurements were made in triplicate and the error bars represents the standard deviation (SD).

3. Results and discussion

3.1. Monolayer formation

QP4VP (strong PE) is cationic regardless of pH while PAA (weak PE) is anionic at pH higher than its pKa (~4.7). Thus, QP4VP and PAA in water may have positive and negative charges on the 5CB, respectively, at pH=7 (the test pH). The GOx enzyme has a PI value of 5.2 which means that GOx has a net negative charge at pH=7, thus, it is reasonable to expect electrostatic interactions between QP4VP and GOx at pH=7. The amount of QP4VP (v_2) was controlled to find the optimum conditions for immobilization of GOx at a fixed v_1 of 200 μL. The reference orientation should be homeotropic because the GOx reaction with glucose induces a homeotropic-to-planar orientational change. Earlier studies showed that QP4VP-coated 5CB in the TEM grid exhibited a homeotropic orientation at a pH range from 2 to ~12 (Omer and Park, 2014). This result was attributed to a large quantity of

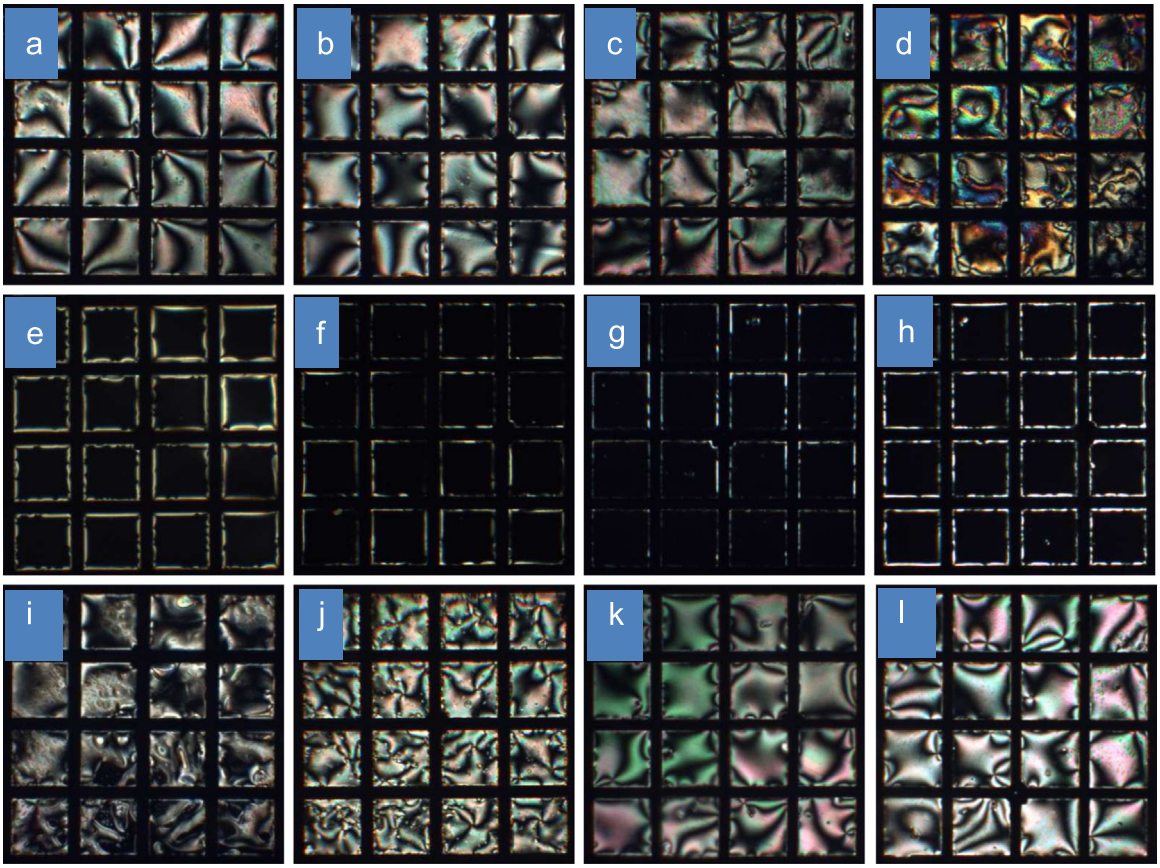

Fig. 1. POM images of the TEM_{mixed} grids at a fixed C_{NaCl}=1 M and v_2= (a) 0, (b) 10, (c) 20, (d) 30, (e) 40, (f) 50, (g) 60, and (h) 80 μL; at a fixed v_2=50 μL and C_{NaCl}=(i) 0.75, (j) 0.5, and (k) 0.2 M; (l) TEM_{PAA} in 1.5 M NaCl.

charges induced by QP4VP that generated an electric field at the 5CB/aqueous interface. Fig. 1a–h shows the POM images (under crossed polarizers) of the TEM_{mixed} grids at different v_2 with a fixed C_{NaCl} of 1 M. At $v_2 \leq$ 30 μL (Fig. 1a–d), a planar orientation of 5CB was observed, while at $v_2 \geq$ 40 μL (Fig. 1e–h), a homeotropic orientation was observed. These results indicate that the homeotropic orientation may be due to high charge density exhibited by the QP4VP PE chains at the 5CB/aqueous interface, and the weak PE, PAA, did not strongly affect the homeotropic orientation under the test conditions.

The counterion salt on the PE greatly affects the orientation of 5CB in the TEM grid; thus, the amount of salt should be controlled. Fig. 1i–k shows the POM images of the TEM_{mixed} at different C_{NaCl} and a fixed v_2 of 50 μL. It has a homeotropic orientation at C_{NaCl} =1 M and v_2=50 μL as discussed in Fig. 1f. At C_{NaCl}=0.75 M (Fig. 1i), a planar orientation was observed along with some dark regions due to sporadic homeotropic orientation. At C_{NaCl}=0.5 and 0.2 M (Fig. 1j–k), the darkness was reduced and a clear planar orientation was observed. These results indicate that sufficient salt is necessary to maintain the homeotropic orientation of 5CB in the TEM grid. However, at v_2=0 μL, the 5CB without QP4VP on the TEM_{mixed} grid (TEM_{PAA}) exhibited a planar orientation even at high C_{NaCl} (1.5 M) (Fig. 1l). Thus, enough QP4VP brush should be coated on the 5CB in the TEM grid with sufficient NaCl in order to obtain the reference homeotropic orientation. Another possibility for generating the homeotropic orientation involves NaCl in the aqueous phase, which can lead to the formation of an electrical double layer via the partitioning of ions from the aqueous phase into the 5CB at the 5CB/aqueous interface. This causes the homeotropic orientation of 5CB in the TEM_{mixed} grid via an electric field induced by the double layer (Carlton et al., 2012). In this work, the C_{NaCl} was fixed at 1 M for a monolayer formation unless otherwise specified.

3.2. Immobilization of GOx

The amount of immobilized GOx (GOx_{imb}) on the TEM grid was ascertained from optical densities determined by UV–vis spectroscopy. Fig. 2a shows the GOx_{imb} as a function of v_2 after injecting a 20 μM GOx solution. The GOx_{imb} increased with increasing v_2, indicating the successful binding of GOx to the QP4VP chains with controllable binding density.

Fig. 2b shows the POM image of the $TEM_{mixed\text{-}GOx}$ after injecting a 20 μM GOx solution into the cell at v_2=40, 50, and 60 μL. Before injection of the GOx solution, the POM images showed a homeotropic orientation, as discussed in the previous section. At v_2=40 and 50 μL (Fig. 2bi, ii), they maintained a homeotropic orientation, while at high v_2 (60 μL), planar orientations were observed (Fig. 2biii). The planar orientation observed with high v_2 might be due to the high amount of immobilized GOx, which caused the planar orientation through electrostatic complex formation leading to a decreased electric field due to neutrality of the complex. Previously, a similar H-P change was observed when PE-coated 5CB in a TEM grid cell was subjected to protein or enzyme solutions above their PI (Omer and Park, 2014). In order to use this surface for glucose detection, an initial homeotropic orientation was required because GOx oxidation of glucose releases protons (H^+) and the protonation of PAA led to planar orientations of the 5CB. A 2 M NaCl solution was used to obtain an initial homeotropic orientation after GOx immobilization in our previous work (Khan and Park, 2013) which might affect the long term stability of the biosensor. However, in the present study, 1 M NaCl was not used

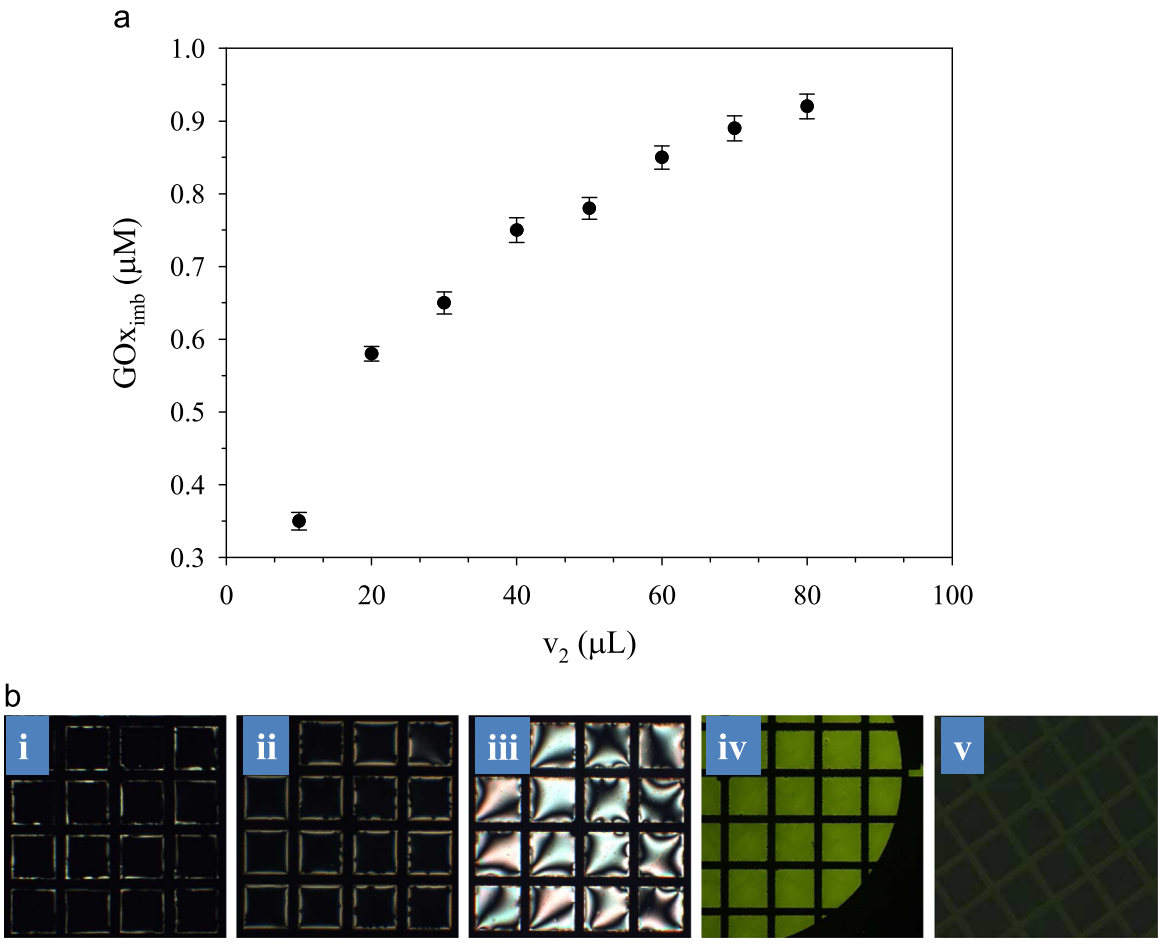

Fig. 2. (a) GOx_{imb} as a function of v_2; (b) POM images of the TEM_{mixed} in a 20 μM GOx solution at v_2=(i) 40, (ii) 50, and (iii) 60 μL; fluorescence microscopy images of (iv) TEM_{mixed}, and (v) TEM_{PAA} after electrostatic immobilization of GOx_{rhd6G} at v_2=50 μL.

during enzyme immobilization and glucose detection, but only during a monolayer formation so that the interactions between the oppositely charged polymer brushes could be avoided. Thus, the present system may have high stability and less interference. The $TEM_{mixed\text{-}GOx}$ with v_2= 50 μL (GOx_{imb}=0.78 μM) was used for all experiments unless otherwise noted.

Fig. 2biv shows the fluorescence microscopy image of the TEM_{mixed} after immobilization of the GOx_{rhd6G} at v_2=50 μL. The green color is uniformly distributed inside the TEM grids while the region outside the TEM grids was almost black, confirming the successful immobilization of GOx. For comparison, TEM_{PAA} was used under the same conditions as with TEM_{mixed}. After washing, a black image (Fig. 2bv) was observed indicating that GOx_{rhd6G} was not immobilized to the PAA chains. This result indicates that the immobilization of GOx is due to the electrostatic attractions between the QP4VP chains and GOx. GOx (PI=5.2) carries negative charges at pH=7 (test pH), thus GOx can be attached only to the cationic QP4VP and not to the PAA.

3.3. Glucose detection and sensitivity

Fig. 3a shows the POM image of the $TEM_{mixed\text{-}GOx}$ grid cell at pH=7 under the crossed polarizer after replacing the aqueous medium in the cell with an 8 mM glucose solution. The initial homeotropic orientation changed to a planar orientation. This H-P change might be due to the release of H^+ ions during the enzymatic oxidation of glucose, reducing the pH in the cell and causing the protonation and shrinkage of the PAA chains. The pH-dependent shrinkage of PAA at the interface could alter the orientational change in the strongly anchored 5CB in the TEM grid

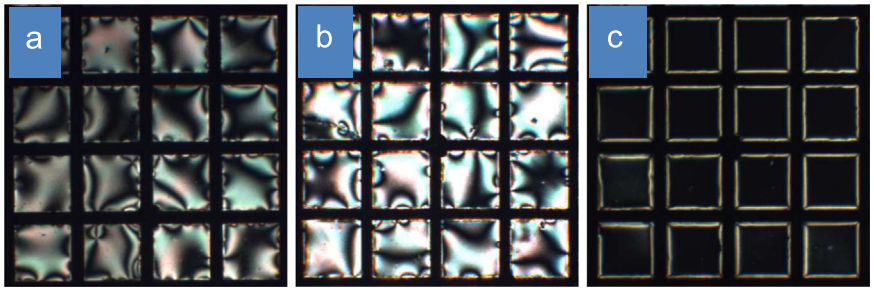

Fig. 3. POM images of the $TEM_{mixed\text{-}GOx}$ in (a) 8 mM glucose solution, and (b) acidic aqueous solution at pH=6, and (c) TEM_{mixed} without immobilized GOx in an 8 mM glucose solution.

cell as reported elsewhere (Lee et al., 2010). The 5CB coated with an amphiphilic block copolymer poly(ethylene imine)-b-*N*-[3-(dimethylamino)-propyl]acrylamide) at the 5CB/aqueous interface undergoes a reversible change in the optical appearance upon alternate exposure to solutions of pH 5 and 9, which was attributed to the protonation and deprotonation states of the hydrophilic chains (Kinsinger et al., 2007). In addition, the varying charge density on the PAA chain led to a change in the 5CB orientation (Lee et al., 2010). An acidic aqueous solution (pH=6) was introduced to determine if the H-P change occurred on lowering the pH. A similar H-P change (Fig. 3b) was observed, confirming that the H-P change by addition of glucose to the $TEM_{mixed\text{-}GOx}$ grid cell was indeed due to a lowered pH resulting from an enzymatic reaction. To confirm that the H-P change was due to the enzymatic reaction of GOx, a 8 mM glucose solution was injected into the flow cell without immobilized GOx (TEM_{mixed}) under otherwise similar conditions. The initial homeotropic orientation was retained (Fig. 3c), indicating that this H-P change was due to GOx reacting with glucose.

Fig. 4 shows the POM images of the $TEM_{mixed\text{-}GOx}$ grid cells with different concentrations (C_0) of glucose solutions. The initial homeotropic orientation did not change at $C_0 \leq 0.4$ mM (Fig. 4a). At $C_0=0.5$ mM (Fig. 4b), a slight brightness appeared in the $TEM_{mixed\text{-}GOx}$ grid cell, and the P-H change became more visible as C_0 increased (Fig. 4c–h). Thus, the $TEM_{mixed\text{-}GOx}$ grid sensor could detect glucose at $C_0 \geq 0.5$ mM. This detection limit is in the similar range with many other reported values. For example, 0.96 mM was reported with a nanocomposite electrode consisting of MWCNTs trapped between the chitosan layers (Monosik et al., 2012). Detection limit of 0.4 mM was observed with GOx immobilized on CNTs in combination with Au and Pt (Chu et al., 2007) and CNTs with a thin plasma-polymerized film (Hoshino et al., 2012). On the other hand, in our previous study, TEM_{PAA} with immobilized GOx had a detection limit of 0.02 mM (Khan and Park, 2013). This low detection limit may be due to the large amount of immobilized GOx (2.6 μM) compared with 0.78 μM of $TEM_{mixed\text{-}GOx}$. However, this electrostatic immobilization of GOx was performed without chemical reactions, and thus is much simpler and more cost effective.

3.4. Kinetics of glucose detection

In accordance with Michel–Levy chart the color of the $TEM_{mixed\text{-}GOx}$ observed by POM under crossed polarizers represents a specific level of retardation. The homeotropic and planar orientations showed black and bright images, respectively, thus, the GI increased as the H-P change progresses. The difference in the optical appearance with increasing C_0 can be an indication of the glucose level in the medium. A frame of the movie represents an image in a short period (4 s) and the GI of each clip can represent the orientation state. Fig. 5a shows GI as a function of time at different C_0. At high C_0 (8 and 5 mM), the GI increased rapidly to the saturation level. The times required to reach half of the saturated level were 180, 120, and 75 s at $C_0=0.5$, 3, and 8 mM, respectively. The saturation level also increased with increasing C_0.

From the GI measurement with time, it was determined that the speed of the change in the optical appearance and its final saturated value were dependent on the amount of glucose present in the cell. Therefore, the precise measurement of the birefringence (Δn) can be quite important for a quantitative measurement of the glucose level. The Δn values of the $TEM_{mixed\text{-}GOx}$ were measured for different C_0, ranging from 0.5 to 42 mM. Fig. 5b shows the change in Δn as a function of C_0. The Δn value increased linearly as C_0 increased until $C_0=11$ mM and became saturated at ~0.08. The linear dynamic range of the $TEM_{mixed\text{-}GOx}$ glucose sensor (until 11 mM) is larger than most of the reported data of 3, 6, 8, 5, and 6.5 mM (Ho et al., 2014; Hwa and Subramani, 2014; Jing-Juan and Hong-Yuan, 2000; Liu and Lin, 2006; Zhai et al., 2013) and we (Khan and Park, 2013) previously reported a value of 2 mM.

The mechanism of the GOx-catalyzed reaction was studied using the linear Michaelis–Menten model as shown in Eq. (1)

$$\frac{C_0}{\Delta n} = \frac{K_m}{\Delta n_{max}} + \frac{1}{\Delta n_{max}} C_0 \quad (1)$$

where Δn_{max} and K_m are the maximum birefringence achieved at the saturated level of the substrate and the Michaelis–Menten constant, respectively. From the intercept and slope of the $C_0/\Delta n$ vs. C_0 plot (Fig. 5c), the K_m and Δn_{max} were 1.67 and 0.084, respectively. The K_m value, 1.67, was smaller than the values of 3.94, 14, and 4.3 mM reported in literature (Jing-Juan and Hong-Yuan, 2000; Malitesta et al., 1990; Zhang et al., 2005).

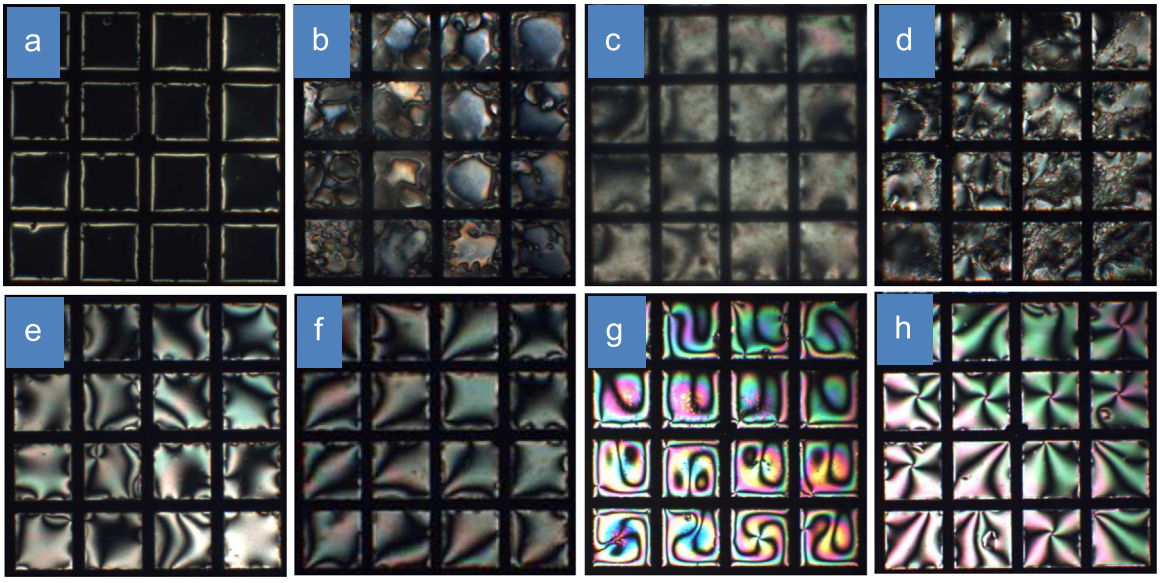

Fig. 4. POM images of $TEM_{mixed\text{-}GOx}$ grid cells in glucose solutions at C_0=(a) 0.4, (b) 0.5, (c) 1, (d) 3, (e) 5, (f) 8, (g) 11, and (h) 16 mM.

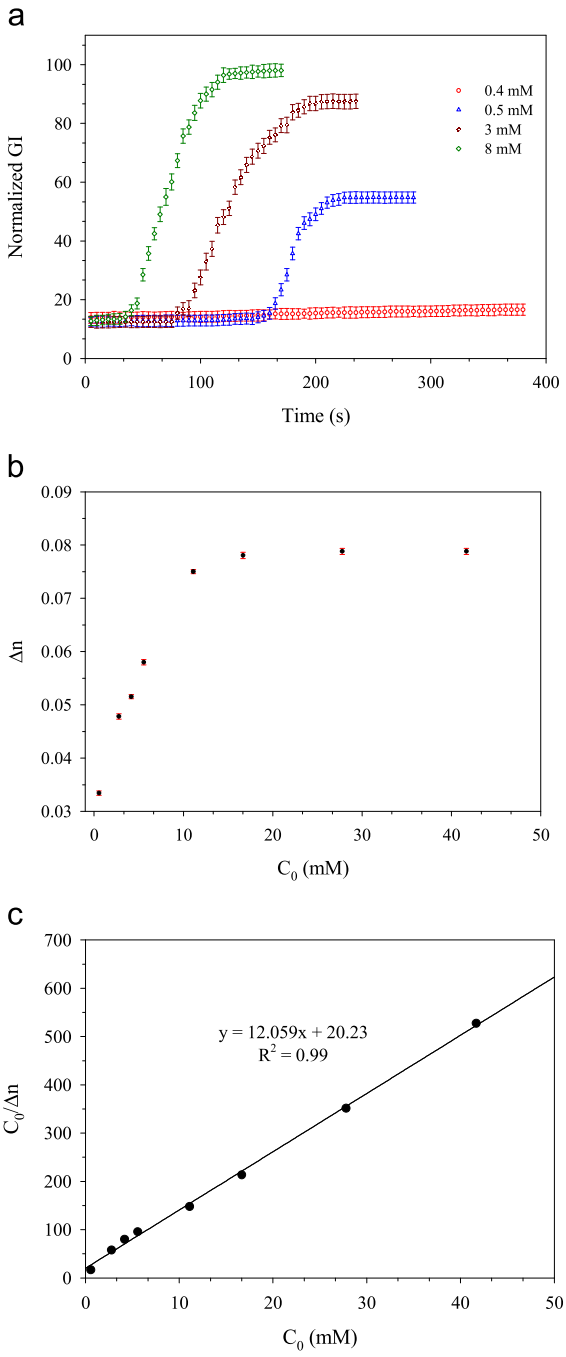

Fig. 5. (a) Normalized GI as a function of time (s), (b) Δn as a function of C_0, and (c) $C_0/\Delta n$ vs. C_0.

However it is larger than our previously reported K_m of 0.32 mM which may be due to the immobilization density of the GOx. The small K_m value suggests that the change in the optical appearance, from the oxidation of glucose by GOx immobilized to the QP4VP chains, in the $TEM_{mixed\text{-}GOx}$ is more sensitive than in other studies. The Δn_{max} is obtain when the upper part of the 5CB that is in contact with aqueous medium is in a perfect parallel orientation and dependent on the hydrophobicity of the OTS-coated glass, brush density and composition of the PE, and the density of the immobilized GOx.

3.5. *Stability and reproducibility of $TEM_{mix\text{-}GOx}$*

Fig. 6a shows the fluorescence emission intensity ratio (I/I_0, I_0 is

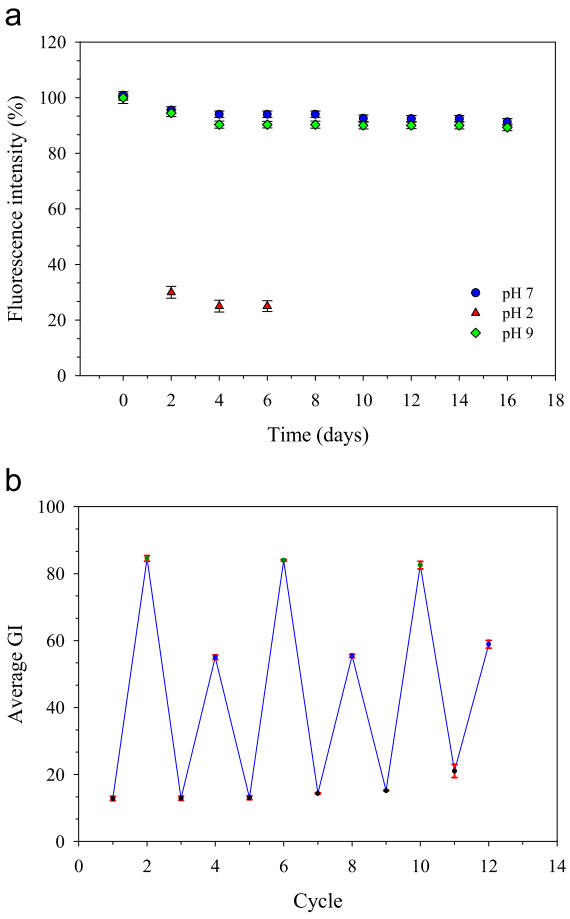

Fig. 6. (a)Fluorescence intensity ratio, I/I_0, in percent as a function of time. (b) Average GI value of the $TEM_{mixed\text{-}GOx}$ sensor with 3 cycles of a reference homeotropic sate after washing, a planar state in a glucose solution at $C_0=8$ mM, a reference homeotropic state after washing, and a planar state in a glucose solution at $C_0=3$ mM.

the initial intensity) at 551 nm in percent as a function of time (Fig. SI 6). At pH=3 (below the PI of GOx), ~75% loss was observed in the fluorescence intensity after four days. However, at pH 7 and 9 (above the PI of GOx), only ~8% loss was observed in four days and no significant loss was noted over 16 days. This result indicates that electrostatic immobilization results in high GOx stability on the QP4VP chains for a long period. In order to test the reproducibility, the $TEM_{mixed\text{-}GOx}$ sensor were alternatively exposed to glucose solution followed by subsequent washing with~10 mL of each PBS buffer (pH=7) and DI water to re-obtain the reference homeotropic state. Fig. 6b shows the averaged GI value of $TEM_{mixed\text{-}GOx}$ glucose sensor with cycles of a reference homeotropic sate after washing, a planar state in a glucose solution at $C_0=8$ mM, a reference homeotropic state again after washing, and a planar state in a glucose solution at $C_0=3$ mM. In each cycle, the GI value was found to be low 14 ± 3 after washing due to the darkened image of the homeotropic orientation, and increased to 84 ± 1 and 54 ± 2 in the 8 and 3 mM glucose solutions, respectively. This result indicates that the $TEM_{mixed\text{-}GOx}$ sensor cell can be used for multiple glucose detections even at different concentrations. In our previous study, the TEM sensor could be utilized only once for glucose detection due to the difficulty in re-obtaining of the reference homeotropic orientation of the 5CB. Thus, the $TEM_{mixed\text{-}GOx}$ sensor has high stability and activity, and capability of multiple usages through electrostatic immobilization of the enzyme (GOx).

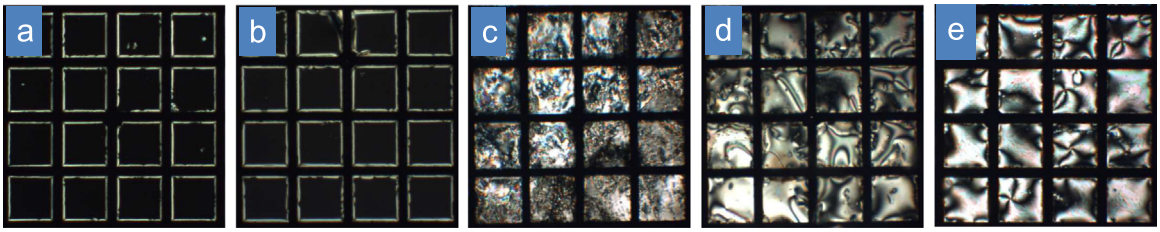

Fig. 7. POM images of $TEM_{mixed\text{-}GOx}$ in a mixture solution with glucose contents of (a) 0, (b) 0.3, (c) 0.5, (d) 2 mM; and (e) mixture solution with unknown contents of glucose.

3.6. *Practical evaluation of $TEM_{mixed\text{-}GOx}$*

Fig. 7 shows the POM images of the $TEM_{mixed\text{-}GOx}$ with the YE/glucose mixtures under crossed polarizers. The initial homeotropic orientation (Fig. 7a) maintained when the aqueous medium in the sensor cell was replaced with a YE/glucose (0.3 mM) mixture (Fig. 7b). A H-P change was observed when a YE/glucose (0.5 mM) mixture was injected in the cell (Fig. 7c). The Δn value obtained from Fig. 7c was 0.0338 ± 0.0003, similar to 0.0334 ± 0.0004 from the pure glucose solution at C_0=0.5 mM (Fig. 4b). The planar orientation became more visible with high content of glucose (2 mM) in the mixture (Fig. 7d). Fig. 7e shows the H-P transition of the $TEM_{mixed\text{-}GOx}$ sensor cell when an unknown content of glucose was used in a mixture solution. The Δn value was found to be 0.055 ± 0.0003 corresponding to the glucose concentration of 4.7 mM according to the linear range of $TEM_{mixed\text{-}GOx}$ in Fig. 5b. In order to check the exact amount of glucose in the YE/glucose mixture, a standard curve ranging C_0=2 to 11 mM was obtained by using a HPLC technique (Fig. SI 7). The YE/glucose mixture solution with unknown glucose content was found to be 4.62 mM from HPLC, similar to that obtained from Δn. Thus, the $TEM_{mixed\text{-}GOx}$ provides enough specificity for glucose detection and quantitative measurement even in a complex mixture.

4. Conclusion

A fast, sensitive, readily made, reliable, cost-effective glucose biosensor was fabricated with a TEM grid filled with 5CB on an OTS-coated glass substrate by coating a monolayer consisting of PAA-*b*-LCP and QP4VP-*b*-LCP on 5CB and physically immobilized GOx at the 5CB/aqueous interface. This TEM grid glucose biosensor was able to detect small amounts of glucose in an aqueous medium and in a complex mixture with a small Michaelis–Menten constant (K_m) value of 1.67 mM, stable for more than 16 days and reproducible for reuse. These performance properties may reveal novel methods to produce an LC biosensor by electrostatic immobilization of enzymes without deteriorating other properties such as long-term stability and sensitivity.

Acknowledgments

This work was supported by the National Research Foundation of Korea (NRF-2011-0020264).

Appendix A. Supplementary material

Supplementary data associated with this article can be found in the online version at http://dx.doi.org/10.1016/j.bios.2015.01.023.

References

Anderson, R., 1997. Elevated intake of supplemental chromium improved glucose and insulin variables in individuals with type 2 diabetes. Diabetes 46, 1786–1791.
Carlton, R.J., Gupta, J.K., Swift, C.L., Abbott, N.L., 2012. Influence of simple electrolytes on the orientational ordering of thermotropic liquid crystals at aqueous interfaces. Langmuir 28 (1), 31–36.
Chu, X., Duan, D., Shen, G., Yu, R., 2007. Amperometric glucose biosensor based on electrodeposition of platinum nanoparticles onto covalently immobilized carbon nanotube electrode. Talanta 71, 2040–2047.
Draper, J., Luzinov, I., Minko, S., Tokarev, I., Stamm, M., 2004. Mixed polymer brushes by sequential polymer addition: anchoring layer effect. Langmuir 20 (10), 4064–4075.
Hanefeld, U., Gardossi, L., Magner, E., 2009. Understanding enzyme immobilisation. Chem. Soc. Rev. 38 (2), 453–468.
Ho, M.L., Wang, J.C., Wang, T.Y., Lin, C.Y., Zhu, J.F., Chen, Y.A., Chen, T.C., 2014. The construction of glucose biosensor based on crystalline iridium(III)-containing coordination polymers with fiber-optic detection. Sens. Actuators B: Chem. 190 (0), 479–485.
Hoshino, T., Sekiguchi, Si, Muguruma, H., 2012. Amperometric biosensor based on multilayer containing carbon nanotube, plasma-polymerized film, electron transfer mediator phenothiazine, and glucose dehydrogenase. Bioelectrochemistry 84, 1–5.
Hwa, K.Y., Subramani, B., 2014. Synthesis of zinc oxide nanoparticles on graphene–carbon nanotube hybrid for glucose biosensor applications. Biosens. Bioelectron. 62 (0), 127–133.
Jain, P., Baker, G.L., Bruening, M.L., 2009. Applications of polymer brushes in protein analysis and purification. Ann. Rev. Anal. Chem. 2 (1), 387–408.
Jing-Juan, X., Hong-Yuan, C., 2000. Amperometric glucose sensor based on coimmobilization of glucose oxidase and Poly(p-phenylenediamine) at a platinum microdisk electrode. Anal. Biochem. 280 (2), 221–226.
Khan, M., Park, S.Y., 2013. Liquid crystal-based proton sensitive glucose biosensor. Anal. Chem. 86 (3), 1493–1501.
Khan, W., Choi, J.H., Kimb, G.M., Park, S.Y., 2011. Microfluidic formation of pH responsive 5CB droplets decorated with PAA-b-LCP. Lab Chip 11, 3493–3498.
Kinsinger, M.I., Sun, B., Abbott, N.L., Lynn, D.M., 2007. Reversible control of ordering transitions at aqueous/liquid crystal interfaces using functional amphiphilic polymers. Adv. Mater. 19, 4208–4212.
Lee, D.Y., Seo, J.M., Khan, W., Kornfield, J.A., Kurjib, Z., Park, S.Y., 2010. pH-responsive aqueous/LC interfaces using SGLCP-b-polyacrylic acid block copolymers. Soft Matter 6, 1964–1970.
Liu, G., Lin, Y., 2006. Amperometric glucose biosensor based on self-assembling glucose oxidase on carbon nanotubes. Electrochem. Commun. 8 (2), 251–256.
Liu, W., Wang, L., Jiang, R., 2012. Specific enzyme immobilization approaches and their application with nanomaterials. Top. Catal. 55 (16–18), 1146–1156.
Malitesta, C., Palmisano, F., Torsi, L., Zambonin, P.G., 1990. Glucose fast-respnse amperometric sensor based on glucose oxidase immobilized in an electropolymerized Poly(o-phenylenediamine) film. Anal. Chem. 62, 2735–2740.
Mateo, C., Palomo, J.M., Fernandez-Lorente, G., Guisan, J.M., Fernandez-Lafuente, R., 2007. Improvement of enzyme activity, stability and selectivity via immobilization techniques. Enzyme Microb. Technol. 40 (6), 1451–1463.
Monosik, R., ansky, M.S., Luspai, K., Magdolen, P., Sturdik, E., 2012. Amperometric glucose biosensor utilizing FAD-dependent glucose dehydrogenase immobilized on nanocomposite electrode. Enzyme Microb. Technol. 50, 227–232.
Nahalka, J., Liu, Z., Chen, X., Wang, P.G., 2003. Superbeads: immobilization in "Sweet" Chemistry. Chem. – A Eur. J. 9 (2), 372–377.
Omer, M., Islam, M., Khan, M., Kim, Y., Lee, J., Kang, I.K., Park, S.Y., 2014a. Liquid crystal-based biosensors using a strong polyelectrolyte-containing block copolymer, poly(4-cyanobiphenyl-4′-oxyundecylacrylate)-b-poly(sodium styrene sulfonate). Macromol. Res. 22 (8), 888–894.
Omer, M., Khan, M., Kim, Y.K., Lee, J.H., Kang, I.K., Park, S.Y., 2014b. Biosensor utilizing a liquid crystal/water interface functionalized with poly(4-cyanobiphenyl-4′-oxyundecylacrylate-b-((2-dimethyl amino) ethyl methacrylate)). Colloids Surfaces B: Biointerfaces 121 (0), 400–408.
Omer, M., Park, S.Y., 2014. Preparation of QP4VP-b-LCP liquid crystal block copolymer and its application as a biosensor. Anal. Bioanal. Chem. 406 (22), 5369–5378.
Osvaldo, N., Oliveira, J., 1992. Langmuir-blodgett films-properties and possible applications. Braz. J. Phys. 22 (2), 60–69.

Price, A.D., Hur, S.-M., Fredrickson, G.H., Frischknecht, A.L., Huber, D.L., 2011. Exploring lateral microphase separation in mixed polymer brushes by experiment and self-consistent field theory simulations. Macromolecules 45 (1), 510–524.
Rad, A.S., Mirabi, A., Binaian, E., Tayebi, H., 2011. A review on glucose and hydrogen peroxide biosensor based on modified electrode included silver nanoparticles. Int. J. Electrochem. Sci. 6, 3671–3683.
Rahman, M.M., Ahammad, A.J.S., Jin, J.H., Ahn, S.J., Lee, J.J., 2010. A comprehensive review of glucose biosensors based on nanostructured metal-oxides. Sensors 10, 4855–4886.
Sassolas, A., Blum, L.J., Leca-Bouvier, B.D., 2012. Immobilization strategies to develop enzymatic biosensors. Biotechnol. Adv. 30 (3), 489–511.
Tan, C., Wang, Q., 2011. Reversible terbium luminescent polyelectrolyte hydrogels for detection of $H2PO^{4-}$ and HSO^{4-} in water. Inorg. Chem. 50 (7), 2953–2956.
Tischer, W., Wedekind, F., 1999. Immobilized enzymes: methods and applications. In: Fessner, W.-D., Archelas, A., Demirjian, D.C., Furstoss, R., Griengl, H., Jaeger, K.E., Morís-Varas, E., Öhrlein, R., Reetz, M.T., Reymond, J.L., Schmidt, M., Servi, S., Shah, P.C., Tischer, W., Wedekind, F. (Eds.), Biocatalysis-From Discovery to Application. Springer, Berlin Heidelberg, pp. 95–126.
Tokarev, I., Minko, S., 2009. Multiresponsive, hierarchically structured membranes: new, challenging, biomimetic materials for biosensors, controlled release, biochemical gates, and nanoreactors. Adv. Mater. 21 (2), 241–247.
Wei, Q., Cai, M., Zhou, F., Liu, W., 2013. Dramatically tuning friction using responsive polyelectrolyte brushes. Macromolecules 46 (23), 9368–9379.
Zhai, D., Liu, B., Shi, Y., Pan, L., Wang, Y., Li, W., Zhang, R., Yu, G., 2013. Highly sensitive glucose sensor based on Pt nanoparticle/polyaniline hydrogel heterostructures. ACS nano 7 (4), 3540–3546.
Zhang, S., Wang, N., Yu, H., Niu, Y., Sun, C., 2005. Covalent attachment of glucose oxidase to an Au electrode modified with gold nanoparticles for use as glucose biosensor. Bioelectrochemistry 67 (1), 15–22.
Zhao, B., Zhu, L., 2009. Mixed polymer brush-grafted particles: a new class of environmentally responsive nanostructured materials. Macromolecules 42 (24), 9369–9383.
Zhu, Z., Garcia-Gancedo, L., Flewitt, A.J., Xie, H., Moussy, F., Milne, W.I., 2012. A critical review of glucose biosensors based on carbon nanomaterials: carbon nanotubes and graphene. Sensors 12, 5996–6022.